

xLSTMAD: A Powerful xLSTM-based Method for Anomaly Detection

Kamil Faber*, Marcin Pietron*, Dominik Żurek*, and Roberto Corizzo†

*AGH University of Krakow, Poland

Email: kfaber@agh.edu.pl, pietron@agh.edu.pl, dzurek@agh.edu.pl

†American University, D.C., USA

Email: rcorizzo@american.edu

Abstract—The recently proposed xLSTM is a powerful model that leverages expressive multiplicative gating and residual connections, providing the temporal capacity needed for long-horizon forecasting and representation learning. This architecture has demonstrated success in time series forecasting, lossless compression, and even large-scale language modeling tasks, where its linear memory footprint and fast inference make it a viable alternative to Transformers. Despite its growing popularity, no prior work has explored xLSTM for anomaly detection. In this work, we fill this gap by proposing xLSTMAD, the first anomaly detection method that integrates a full encoder-decoder xLSTM architecture, purpose-built for multivariate time series data. Our encoder processes input sequences to capture historical context, while the decoder is devised in two separate variants of the method. In the forecasting approach, the decoder iteratively generates forecasted future values xLSTMAD-F, while the reconstruction approach reconstructs the input time series from its encoded counterpart xLSTMAD-R. We investigate the performance of two loss functions: Mean Squared Error (MSE), and Soft Dynamic Time Warping (SoftDTW) to consider local reconstruction fidelity and global sequence alignment, respectively. We evaluate our method on the comprehensive TSB-AD-M benchmark, which spans 17 real-world datasets, using state-of-the-art challenging metrics such as VUS-PR. In our results, xLSTM showcases state-of-the-art accuracy, outperforming 23 popular anomaly detection baselines. Our paper is the first work revealing the powerful modeling capabilities of xLSTM for anomaly detection, paving the way for exciting new developments on this subject. Our code is available at: <https://github.com/Nyderx/xlstmad>.

Index Terms—xLSTM, anomaly detection, deep learning, time series

I. INTRODUCTION

Anomaly detection in multivariate time series is a vital task across domains such as industrial monitoring, cybersecurity, human activity recognition, and space system diagnostics. While statistical techniques and classical machine learning models remain strong baselines, deep learning methods have emerged as powerful alternatives due to their ability to model complex temporal dependencies and high-dimensional patterns. Recent benchmarks like TSB-AD [1] reveal that even simple neural architectures (e.g., CNNs [2], LSTMs [3]) can outperform more complex Transformer variants [4], [5] in anomaly detection tasks—particularly in multivariate settings where expressive temporal modeling is key.

Most state-of-the-art deep learning approaches fall into two broad categories: reconstruction-based models (e.g., autoencoders, VAEs) that detect anomalies through high reconstruc-

tion error, and prediction-based models (e.g., LSTMs) that forecast future behavior and identify deviations. However, these models often struggle to balance long-term memory, fine-grained temporal resolution, and computational efficiency [1].

The recently proposed xLSTM architecture offers a promising research direction [6]. As a generalization of LSTM, it combines depth-wise convolutions, residual connections, and multi-scale gating mechanisms in a stackable, efficient structure. xLSTM has demonstrated success in time series forecasting [7], lossless compression [8], and even large-scale language modeling [9], where its linear memory footprint and fast inference make it a viable Transformer alternative. Despite its growing popularity, no prior work has explored xLSTM for anomaly detection.

In this work, we fill this gap by proposing xLSTMAD, the first encoder-decoder xLSTM model for multivariate time series anomaly detection. Our architecture is purpose-built: an encoder processes input sequences to capture historical context, while a decoder is devised in two separate variants. In the forecasting approach, the decoder iteratively generates forecasted future values xLSTMAD-F, while the reconstruction approach reconstructs the input time series from its encoded counterpart xLSTMAD-R. We investigate the performance of two loss functions: Mean Squared Error (MSE), and Soft Dynamic Time Warping (SoftDTW), with the intention to consider local reconstruction fidelity and global sequence alignment, respectively.

To rigorously evaluate our approach, we leverage the TSB-AD-M benchmark [1], a comprehensive suite of 17 real-world datasets ranging from industrial control systems (e.g., SWaT, SMD) to spacecraft telemetry (e.g., SMAP, MSL) and human activity monitoring (e.g., OPP), designed to create extremely challenging conditions that are useful to assess the effectiveness of diverse models in diverse conditions. Our results show that the xLSTM encoder-decoder architecture achieves superior performance compared to classical and modern baselines.

The contributions of this work can be summarized as:

- We propose \times LSTMAD, the first encoder-decoder architecture based entirely on xLSTM blocks for multivariate time series anomaly detection, leveraging its efficient recurrence, convolutional depth, and long-range memory.
- The proposed \times LSTMAD method integrates residual connections, depthwise convolutions, and a hybrid stacking of mLSTM and sLSTM blocks. The model is designed to balance expressiveness and stability, with selective placement of gating and feedforward components.
- We propose and evaluate two variants of \times LSTMAD: *forecasting-based* anomaly scoring \times LSTMAD-F, and *reconstruction-based* \times LSTMAD-R, allowing flexibility in how the decoder’s outputs are used to identify abnormal behavior depending on the domain or data characteristics.
- We investigate the performance of two loss functions: *Mean Squared Error (MSE)* and *Soft Dynamic Time Warping (SoftDTW)*, which capture pointwise deviations and temporal distortions, crucial for detecting subtle or delayed anomalies, respectively.
- We evaluate our method on 17 real-world datasets from the TSB-AD-M benchmark, the most challenging time series anomaly detection benchmark covering diverse domains such as industrial control, spacecraft telemetry, and human activity, and resorting to comprehensive metrics such as VUS-PR, in addition to more traditional metrics.

II. BACKGROUND

A. Time series anomaly detection

Anomaly detection in time series encompasses a range of classical and modern methods. Traditional statistical approaches assume an underlying generative model of normal behavior and use statistical tests or thresholds to flag outliers. For example, one may fit an ARIMA or seasonal model and then apply hypothesis tests on residuals [10], [10], [11].

In the deep learning era, reconstruction-based models have become popular for time-series anomaly detection. Autoencoders (AEs) are neural networks trained to reconstruct input sequences, and anomalies are identified by high reconstruction error. Sakurada and Yairi [12] showed that even simple AEs can outperform linear PCA for detecting anomalies in multivariate time series. Modern variants (e.g., denoising AEs, convolutional AEs) follow the same principle.

Generative deep models explicitly learn the probability distribution of normal time-series data. Variational autoencoders (VAEs) and GANs are common in this class. For example, OmniAnomaly [13] uses a recurrent VAE with planar normalizing flows to model multivariate time series.

Recently, transformer and attention-based architectures have been applied to anomaly detection. Transformers process the entire sequence via self-attention, capturing long-range dependencies without explicit recurrence. The Anomaly Transformer [5] uses self-attention to learn pairwise associations between time points: it models both “prior” (local Gaussian-weighted) and “series” (learned self-attention) associations,

and anomalies are detected when these expected associations are disrupted. Related models like TranAD [4] demonstrate that transformer-based models can differentiate anomalies by their deviant attention patterns and reconstruction discrepancies.

B. \times LSTM

xLSTM is rapidly gaining traction in different tasks. The most natural application as a direct successor of the LSTM architecture is in time series prediction tasks. The work in [14] proposed an advanced stock price prediction model based on xLSTM, with the aim of enhancing predictive accuracy in both short and long term periods. Experimental results with multiple stocks showed that xLSTM consistently outperforms LSTM across all stocks and time horizons, and this gap widens as the prediction period extends.

The success of xLSTM in time series prediction led researchers to make efforts towards its adaptation towards other tasks, data types, and domains. An example is lossless compression based on neural networks. The work in [8] propose a novel lossless compressor with two compression stages: parallel expansion mapping, which maps redundant pieces in multi-source data into unused alphabet values, and compression through an xLSTM model with a Deep Spatial Gating Module (DSGM). Authors in [15] introduce Vision-LSTM (ViL), an adaptation of xLSTM building blocks to computer vision. The architecture provides a stack of xLSTM blocks in which odd blocks process the sequence of patch tokens from top to bottom while even blocks go from bottom to top. The proposed model achieved strong classification performance in transfer learning and segmentation tasks, showing promise for further deployment of xLSTM in computer vision architectures. Similarly, LLMs built on the xLSTM architecture have emerged as a viable alternative to Transformers, due to a linear relationship between sequence length and compute requirements, as well as the constant memory usage. The authors in [9] introduced xLSTM 7B, a 7-billion-parameter LLM with targeted optimizations for fast and efficient inference. The model was able to achieve performance on downstream tasks similar to popular models such as Llama- and Mamba-based LLMs with a significantly faster inference speed [9].

Despite the recent success of xLSTM in many contexts, to the best of our knowledge, no study thus far has explored its capabilities for time series anomaly detection. The goal of our paper is to address this gap.

C. TSB-AD anomaly detection benchmark

In the original TSB-AD study [1], a comprehensive collection of 40 time-series anomaly detection algorithms is leveraged to compare statistical, neural network-based, and the latest foundation model-based methods. Extensive experiments conducted on the TSB-AD benchmark led to relevant insights. First, statistical methods generally exhibit strong and consistent performance. In contrast, neural network-based models often fall short of their reputed superiority, though they still

perform competitively in detecting point anomalies and handling multivariate time series. Moreover, simple architectures like CNNs and LSTMs tend to outperform more sophisticated designs such as advanced Transformer variants.

Even though CNN [2] and OmniAnomaly [13] display the strongest performance on multivariate datasets, the analysis provided by the TSB-AD benchmark highlights the need for more expressive models in complex multivariate settings.

III. METHOD

In this section, we describe our proposed \times LSTMAD method. The model architecture is shown in Figure 1. In the following, we first formally introduce \times LSTM, the foundational layer used in our architecture. Second, we showcase the model architecture in terms of its constituent blocks. Third, we devise the two variants of our method: forecasting \times LSTMAD-F and reconstruction-based \times LSTMAD-R. Finally, we explain the two losses adopted to train the model architecture.

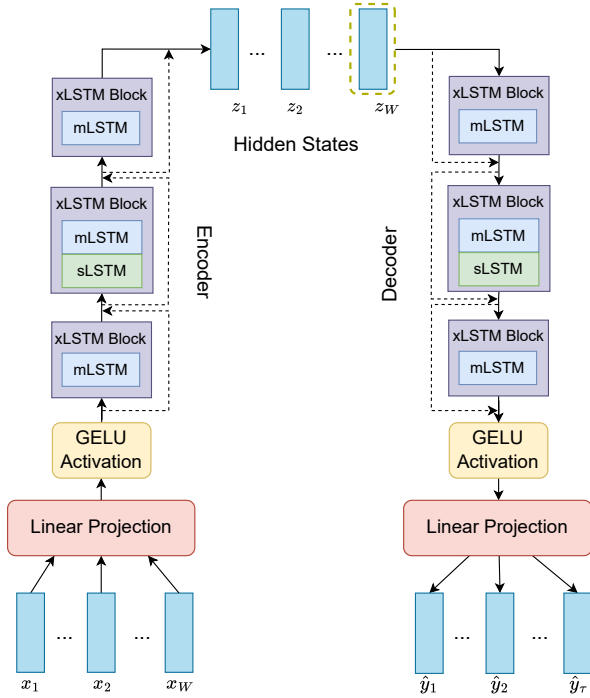


Fig. 1. Proposed \times LSTMAD Encoder-Decoder model architecture. Input data is organized as multivariate time series x_1, x_2, \dots, x_W , where W is the window size. The data fed to the Encoder is processed into hidden states z_1, z_2, \dots, z_W through linear projection, GELU activation, and multiple residually stacked \times LSTM blocks. The Decoder generates reconstructions \times LSTMAD-R or forecasts \times LSTMAD-F, which are then leveraged in the computation of anomaly scores. Dashed lines denote residual connections between stacked blocks.

A. \times LSTM

The *Extended Long Short-Term Memory (xLSTM)* [6] model architecture presents a significant advancement over the classical LSTM by addressing three major limitations: *i)* inability to revise past storage decisions, *ii)* limited memory capacity due to scalar-valued cell states, and *iii)* lack of parallelizability

stemming from sequential hidden-to-hidden state dependencies. Specifically, a standard LSTM updates its memory cell as:

$$c_t = f_t c_{t-1} + i_t z_t, \quad (1)$$

where f_t, i_t are sigmoid gates and z_t is the candidate memory input. In contrast, \times LSTM introduces *exponential gating*, where gates can take the form:

$$i_t = \exp(\tilde{i}_t), \quad f_t = \exp(\tilde{f}_t), \quad (2)$$

allowing for a sharper and more dynamic weighting of memory contributions. A normalization mechanism via a *normalizer state* n_t ensures numerical stability:

$$n_t = f_t n_{t-1} + i_t, \quad \tilde{h}_t = \frac{c_t}{n_t}. \quad (3)$$

This behavior enables effective revision of prior information. We argue that this property is beneficial for detecting anomalous patterns that require continual memory updates as new evidence arrives.

Memory Mixing: \times LSTM architecture introduces a new **sLSTM** cell with a scalar memory, a scalar update, and memory mixing. As exponential activation functions can lead to large values that cause overflows, the sLSTM cell includes an additional state m_t leveraged to stabilize the gates. Moreover, sLSTM leveraged a new memory mixing approach, in which a hidden state vector is connected to the memory cell and input, forgetting, and output gates. Moreover, while sLSTM can have multiple heads, the memory mixing is adopted only within each head, not across different heads.

Matrix-Valued Memory: To overcome the bottleneck of scalar memory cells, \times LSTM introduces the **matrix LSTM (mLSTM)** with a memory update rule:

$$C_t = f_t C_{t-1} + i_t v_t k_t^\top, \quad (4)$$

where v_t and k_t are value and key vectors, respectively. This outer-product update—similar in spirit to associative memories—enables richer storage and retrieval capabilities, which are crucial for handling high-dimensional or temporally dispersed anomalies in time series.

Parallelizable Design: Unlike traditional LSTMs, the mLSTM variant included in \times LSTM removes hidden-to-hidden connections, making it fully parallelizable. This addresses the LSTM's sequential bottleneck and improves scalability, allowing deployment in large-scale, real-time anomaly detection systems.

These upgrades are particularly relevant for anomaly detection in time series data, where models must: *i)* retain and revise long-range dependencies (enabled by exponential gating), *ii)* capture complex, multi-dimensional patterns (through matrix-valued memory), and *iii)* scale efficiently to long sequences and high-frequency streams (via parallelizable updates). \times LSTM thus provides a more expressive, adaptive, and efficient sequence modeling backbone for anomaly detection tasks compared to conventional LSTMs. However, thus far, no research on \times LSTM has been carried out in the realm of

anomaly detection. The main goal of our study is to investigate the effectiveness of xLSTM models for time series anomaly detection tasks.

B. Proposed model architecture

Given an input time series $\mathbf{X} \in \mathbb{R}^{B \times W \times F}$, where B is the batch size, W is the context (window) length, and F is the input features dimension, the model processes the sequence through three stages described below.

1. *Input Projection*: The input is projected into a D -dimensional embedding space:

$$\mathbf{H}_0 = \phi(\mathbf{X}\mathbf{W}_p + \mathbf{b}_p) \in \mathbb{R}^{B \times W \times D} \quad (5)$$

where $\mathbf{W}_p \in \mathbb{R}^{F \times D}$ and ϕ is a non-linear activation (e.g., GELU).

2. *Encoder: Residual xLSTM Blocks*: xLSTM encoder xLSTM_{enc} is built of 3 xLSTM blocks, each of which consists of an mLSTM layer with an optional sLSTM layer. For simplicity, in the following, we describe how a single xLSTM block of xLSTM_{enc} is defined.

Let the encoder contain L stacked blocks, indexed by $\ell = 1, \dots, L$. For each layer ℓ , the output of an mLSTM layer is defined as:

$$\mathbf{H}_\ell^{(m)} = \text{mLSTMCell}_\ell(\text{Conv1D}_8(\mathbf{H}_{\ell-1})) \quad (6)$$

where Conv1D_8 corresponds to one dimensional convolutional layer with kernel size = 8.

If sLSTM layer is included in the block ℓ , we define its output as:

$$\mathbf{H}_\ell^{(s)} = \text{sLSTMCell}_\ell(\text{Conv1D}_4(\mathbf{H}_\ell^{(m)})) \quad (7)$$

$$\mathbf{H}_\ell^{(f)} = \text{FFN}_\ell(\mathbf{H}_\ell^{(s)}) \quad (8)$$

The output of a single xLSTM block leverages the output of the sLSTM layer and the residual connection:

$$\mathbf{H}_\ell = \mathbf{H}_{\ell-1} + \mathbf{H}_\ell^{(f)} \quad (9)$$

3. *Decoder: Autoregressive Forecasting*: Following the encoding stage, the decoding stage generates forecasts for subsequent time steps xLSTMAD-F or multi-dimensional reconstructions xLSTMAD-R , depending on the preferred variant.

The decoding stage includes a decoder xLSTM_{dec} consisting of multiple xLSTM blocks, similar to xLSTM_{enc} defined above.

First, the decoder state is initialized from the last encoder timestep:

$$\mathbf{h}_0 = \mathbf{H}_L[:, -1, :] \in \mathbb{R}^{B \times D} \quad (10)$$

Second, predictions are generated for $t = 1, \dots, \tau$:

$$\mathbf{h}_t = \text{xLSTM}_{dec}(\mathbf{h}_{t-1}) \quad (11)$$

where τ is equal to the forecasting horizon in xLSTMAD-F and to the original sequence size in reconstruction variant xLSTADM-R .

Finally, a GELU activation function ϕ is applied to the decoded hidden state, and the result is projected into the F -dimensional feature space:

$$\hat{\mathbf{y}}_t = \phi(\mathbf{z}_t \mathbf{W}_o + \mathbf{b}_o) \in \mathbb{R}^{B \times F} \quad (12)$$

The final output sequence can be formalized as:

$$\hat{\mathbf{Y}} = [\hat{\mathbf{y}}_1, \hat{\mathbf{y}}_2, \dots, \hat{\mathbf{y}}_\tau] \in \mathbb{R}^{B \times \tau \times F} \quad (13)$$

C. Anomaly detection strategies

Let us recall that for a given time step t , the model takes as input the historical window of size W :

$$\mathbf{X}_t^{(W)} = [\mathbf{x}_{t-W+1}, \dots, \mathbf{x}_t] \in \mathbb{R}^{W \times F} \quad (14)$$

We propose two anomaly detection approaches: Forecasting xLSTMAD-F and Reconstruction xLSTMAD-R .

1) *Forecasting xLSTMAD-F*: For a given time step t , the model takes as input the historical window $\mathbf{X}_t^{(W)}$ and generates forecasts for the next p steps, where p defines the forecasting horizon:

$$\hat{\mathbf{X}}_{t+1:t+p} = f_\theta(\mathbf{X}_t^{(W)}) \in \mathbb{R}^{p \times D} \quad (15)$$

The ground truth for the prediction is:

$$\mathbf{X}_{t+1:t+p} = [\mathbf{x}_{t+1}, \mathbf{x}_{t+2}, \dots, \mathbf{x}_{t+p}] \quad (16)$$

In principle, using multiple prediction time steps should allow the model to leverage the smoothness of multi-step-ahead forecasts, with a potential improved anomaly detection robustness. However, this setup assumes that anomalies will be detected with some delay, since, after prediction, the computation of the anomaly score requires the next p time steps. Therefore, the choice of forecasting horizon p may depend on a specific domain and requirements.

The pointwise prediction error can be quantified using the Mean Squared Error (MSE) across the prediction horizon and all dimensions:

$$\mathcal{L}_{\text{pred}}(t) = \frac{1}{p \cdot D} \sum_{i=1}^p \sum_{j=1}^D (x_{t+i,j} - \hat{x}_{t+i,j})^2 \quad (17)$$

This prediction error is used directly as the raw anomaly score at time $t + p$, indicating how well the model's forecast matches the actual future behavior, thus enabling a threshold-free evaluation setup.

The forecasting-based approach enables the model to directly learn temporal dynamics and causal dependencies, making it effective for detecting subtle deviations from expected future behavior. Such deviations often signal contextual or collective anomalies in the sequence.

2) *Reconstruction xLSTMAD-R*: In the reconstruction-based paradigm, we train a model to learn a compressed representation of past observations and reconstruct them as accurately as possible.

A reconstruction model g_ϕ (e.g., an autoencoder) is trained to map each window $\mathbf{X}_t^{(W)}$ to a reconstruction $\hat{\mathbf{X}}_t^{(W)}$:

$$\hat{\mathbf{X}}_t^{(W)} = g_\phi(\mathbf{X}_t^{(W)}) \in \mathbb{R}^{W \times D} \quad (18)$$

The reconstruction loss at time t is defined as the Mean Squared Error (MSE) between the input and its reconstruction:

$$\mathcal{L}_{\text{recon}}(t) = \frac{1}{w \cdot D} \sum_{i=1}^w \sum_{j=1}^D (x_{t-W+i,j} - \hat{x}_{t-W+i,j})^2 \quad (19)$$

In our work, the raw anomaly scores, i.e., reconstruction error, predicted by the model are directly exploited for evaluation, overcoming the need for thresholding schemes to extract binary predictions. High reconstruction error values indicate points where the model fails to accurately reproduce the input, suggesting potential anomalies.

D. Loss functions

We experiment with different loss functions specifically designed for time series data. Considering the two anomaly detection approaches devised above, this leads to four separate configurations in our study.

1) *Mean Squared Error*: This standard approach computes the loss based on the Mean Squared Error between the predicted sequence $\hat{\mathbf{X}}$ obtained via the xLSTM decoder and the ground truth input sequence \mathbf{X} , as shown in Eq. 17 xLSTMAD-F and Eq. 19 xLSTMAD-R.

2) *Phase-Aware Shape Consistency Loss via SoftDTW*: To address the limitations of pointwise losses such as MSE in time series modeling, we incorporate a *Soft Dynamic Time Warping (SoftDTW)* loss [16]. Unlike traditional losses that penalize exact time-aligned discrepancies, SoftDTW enables differentiable sequence alignment, allowing for temporal shifts and warping, which are common in multivariate time series domains such as sensor networks, human activity recognition, and ECG signal monitoring.

Given an input sequence $\mathbf{X} \in \mathbb{R}^{T \times F}$ and its forecasted or reconstructed counterpart $\hat{\mathbf{X}} \in \mathbb{R}^{T' \times F}$, we first define a cost matrix $C \in \mathbb{R}^{T \times T'}$ where each entry is the squared Euclidean distance between time step vectors:

$$C_{i,j} = \|\mathbf{X}_i - \hat{\mathbf{X}}_j\|^2 \quad \text{for } i = 1, \dots, T; j = 1, \dots, T' \quad (20)$$

The SoftDTW loss is then computed using a smooth approximation of the classical Dynamic Time Warping cost, defined recursively using the *softmax* operator:

$$\mathcal{D}_\gamma(i, j) = C_{i,j} + \gamma \cdot \text{softmax} \begin{pmatrix} \mathcal{D}_\gamma(i-1, j) \\ \mathcal{D}_\gamma(i, j-1) \\ \mathcal{D}_\gamma(i-1, j-1) \end{pmatrix} \quad (21)$$

where $\gamma > 0$ is a smoothing parameter, and the *softmax* function is defined as:

$$\text{softmax}(a_1, a_2, a_3) = -\gamma \cdot \log \left(\exp \left(-\frac{a_1}{\gamma} \right) + \exp \left(-\frac{a_2}{\gamma} \right) + \exp \left(-\frac{a_3}{\gamma} \right) \right) \quad (22)$$

The final SoftDTW loss is the value of $\mathcal{D}_\gamma(T, T')$, which reflects the smoothed alignment cost between \mathbf{X} and $\hat{\mathbf{X}}$:

$$\mathcal{L}_{\text{SoftDTW}} = \mathcal{D}_\gamma(T, T') \quad (23)$$

This formulation preserves differentiability with respect to both inputs and outputs, allowing seamless integration into gradient-based optimization. Moreover, by accounting for local temporal misalignments, SoftDTW provides a more robust metric for sequence similarity, especially in tasks such as anomaly detection, where phase variation may not correspond to actual anomalies.

IV. EXPERIMENTAL SETUP

In our experiments, we leverage the recently proposed comprehensive TSB-AD benchmark, which tackles the multiple issues affecting previous anomaly detection evaluations, such as flawed datasets, biased evaluation measures, and inconsistent benchmarking practices [1]. The benchmark includes a diverse set of multivariate time series datasets, with different underlying domain characteristics. This variety allows us to provide a comprehensive evaluation across various real-world challenges.

A. Metrics

Popular metrics in anomaly detection include threshold-based metrics (**Precision**, **Recall**, **F1-Score**) that allow the evaluation of the various aspects of the performance of the model. A commonly used extension of F1-Score is the **PA-F1** metric, which utilizes point adjustment on predictions. F1 has also been extended to consider the sequential nature of time series. The **event-based F1** that considers each anomaly segment as a distinct event, contributing exactly once as a true positive or a false negative. On the other hand, the **R-based-F1** extends traditional evaluation metrics by incorporating components such as existence reward, overlap reward, and a cardinality factor. Moreover, **Affiliation-F1** emphasizes the temporal closeness between predicted and actual anomaly segments, quantifying their alignment based on the temporal distance [1]. However, the values of these metrics vary significantly depending on the choice of anomaly threshold.

To evaluate a model using its corresponding anomaly scores, the Area Under the Receiver Operating Characteristics curve (**AUC-ROC**) [17] is a much more desirable metric. It is defined as the area under the curve corresponding to TPR on the y-axis and FPR on the x-axis, as the threshold of the anomaly score varies. Another metric following a similar idea is the Area Under the Precision-Recall curve (**PR-AUC** [18]), which leverages Precision on the y-axis and Recall on the x-axis. Although these metrics overcome the limitation of threshold-based metrics, they only gather point-based anomalies.

Two desiderata in time series are *range detection*, i.e., the anomaly detection algorithm should ideally detect every point in the anomalous sequence, and *existence detection*, i.e., the detection of a tiny segment of one anomalous sequence is preferred rather than missing out on the whole sequence. To address this problem, a promising direction was recently proposed in [19], where the AUC was extended for range-based anomaly detection.

Volume Under the Surface (VUS) extends the mathematical model of Range-AUC measures by varying the window length, making the VUS family of measures truly parameter-free. This formulation also leads to an increased robustness to lag, noise, and anomaly cardinality ratio, as well as a high separability between accurate and inaccurate methods and consistency.

VUS-ROC and **VUS-PR** build a surface of TPR, FPR based on varying window lengths. The volume under the surface then represents a measure of AUC for various windows. Since many time series anomaly detection models are sensitive to different window-length setups, the adoption of VUS enables a more fair and robust estimation and comparison of model performance. Due to these powerful properties, we focus our experiments on the VUS family metrics while including the other classical metrics for completeness. A more formal definition of the VUS family of measures can be found in [19].

B. Reproducibility guidelines

We follow the exact guidelines provided by the authors of the TSB-AD benchmark to ensure reproducibility and fair comparison of future methods. Although we provide a brief description of the evaluation scheme in the following, a detailed description and statistics can be found in the original paper [1]. The hyperparameter tuning set consists of 15% of each dataset, while the rest of the data is used to train and evaluate anomaly detection methods. The evaluation data is divided into 180 time series across 17 datasets. Each evaluation time series is then divided into training and test data sets. The datasets, along with information on all the splits, are available in the original TSB-AD repository: <https://github.com/TheDatumOrg/TSB-AD/>.

It should be noted that a single set of tuned hyperparameters is selected for all datasets rather than tuning hyperparameters specifically for each dataset. Such a decision improves the analysis of the models' robustness but makes it more challenging to achieve high results across all datasets.

The hyperparameters search space for our methods includes:

- \times LSTMAD-R: window size: {15, 25, 50}, learning rate: {0.005, 0.001, 0.0008}, embedding dimensionality: {20, 40}.
- \times LSTMAD-F: window size: {15, 25, 50}, learning rate: {0.005, 0.001, 0.0008}, embedding dimensionality: {20, 40}, forecasting horizon: {1, 5, 15}.

We selected the hyperparameters that yield the highest value of the VUS-PR metric achieved on the tuning set. The final hyperparameters are presented in Table I.

The evaluation set is divided into 180 time series that are then split into training and test parts. As a result, our experiments included 720 training and test executions for our \times LSTMAD-R and \times LSTMAD-F methods with two losses (MSE and SoftDTW). All experiments were performed on a single Nvidia GH200 GPU. Our code is available at <https://github.com/Nyderx/xlstmad>.

TABLE I
FINAL HYPERPARAMETERS FOR ALL METHODS: WINDOW SIZE (WIN. SIZE), LEARNING RATE (LR), EMBEDDING DIMENSIONALITY (EMBED. DIM), FORECASTING HORIZON (HORIZON). NA = NON APPLICABLE

Method	Win. Size	LR	Embed. Dim	Horizon
\times LSTM-F (MSE)	50	0.0008	20	5
\times LSTM-F (DTW)	25	0.005	20	5
\times LSTM-R (MSE)	50	0.005	40	NA
\times LSTM-R (DTW)	25	0.001	20	NA

V. RESULTS DISCUSSION

Our experiments are aimed at answering the following research questions:

- **RQ1.** Do our proposed \times LSTMAD strategies exhibit superior performance on the challenging TSB-AD-M benchmark compared to state-of-the-art baselines in anomaly detection?
- **RQ2.** Does \times LSTMAD consistently outperform other methods in a fine-grained comparison that considers single datasets?

We recall that challenging experimental choices originating from the adopted benchmark may impact the performance of each model. Specifically, hyperparameter tuning is performed just once, selecting a single hyperparameter configuration that achieves the best results across all datasets. Another observation is that VUS-PR and VUS-ROC are very challenging metrics. Since they evaluate model performance across multiple time periods, they exacerbates the evaluation for all models, yielding significantly lower results than ROC-AUC.

In the following discussions, we focus on comparisons between our proposed method and two baselines: CNN [2] and LSTMAD [3]. While CNN is relevant since it achieved the best performance in the TSB-AD benchmark [1], LSTMAD is a natural competitor since it is based on LSTM, the predecessor of \times LSTM. Moreover, to support the interpretation of experimental results, we provide a Random model that simply returns a random anomaly score in the range from 0 to 1. This allows us to set realistic expectations for VUS-based metric values for non-random anomaly detection methods.

A. \times LSTMAD results across all datasets

Table II shows that all \times LSTMAD variants outperform state-of-the-art baselines, especially in terms of the most challenging VUS-PR metric. The best performing \times LSTMAD-R with MSE loss outperforms current state-of-the-art results, achieved by CNN, OmniAnomaly, and LSTMAD, by almost 20% (0.37 vs 0.31). In particular, it performs 370% better than the random model (0.37 vs. 0.10).

While \times LSTMAD-R presents better results than other variants in terms of VUS-PR (0.37), the proposed \times LSTMAD-F model with MSE loss consistently outperforms a broad range of classical and deep learning baselines across all metrics. It achieves the highest AUC-PR (0.35), AUC-ROC (0.74), VUS-ROC (0.77), Affiliation-F1 (0.89), PA-F1 (0.85), Event-based-F1 (0.70), R-Based-F1 (0.42), and Standard-F1 (0.40),

TABLE II

SUMMARY COMPARISON OF OUR PROPOSED METHOD WITH 23 COMPETITORS ACROSS 180 TIME-SERIES ORIGINATING FROM 17 DATASETS IN TERMS OF MULTIPLE METRICS. THE BEST-PERFORMING METHOD FOR EACH METRIC IS MARKED IN BOLD.

Method	VUS-PR	VUS-ROC	AUC-PR	AUC-ROC	Standard-F1	PA-F1	Event-based-F1	R-based-F1	Affiliation-F1
xLSTMAD-F (MSE)	0.35	0.77	0.35	0.74	0.40	0.85	0.70	0.42	0.89
xLSTMAD-F (SoftDTW)	0.34	0.76	0.35	0.73	0.40	0.83	0.67	0.41	0.88
xLSTMAD-R (MSE)	0.37	0.72	0.32	0.68	0.38	0.53	0.45	0.36	0.82
xLSTMAD-R (SoftDTW)	0.36	0.72	0.31	0.68	0.37	0.57	0.48	0.35	0.82
RandomModel	0.10	0.59	0.05	0.50	0.09	0.71	0.10	0.10	0.69
CNN [2]	0.31	0.76	0.32	0.73	0.37	0.78	0.65	0.37	0.87
OmniAnomaly [13]	0.31	0.69	0.27	0.65	0.32	0.55	0.41	0.37	0.81
PCA	0.31	0.74	0.31	0.7	0.37	0.79	0.59	0.29	0.85
LSTMAD [3]	0.31	0.74	0.31	0.7	0.36	0.79	0.64	0.38	0.87
USAD [20]	0.3	0.68	0.26	0.64	0.31	0.53	0.4	0.37	0.8
AutoEncoder [12]	0.3	0.69	0.3	0.67	0.34	0.6	0.44	0.28	0.8
KMeansAD [21]	0.29	0.73	0.25	0.69	0.31	0.68	0.49	0.33	0.82
CBLOF [22]	0.27	0.7	0.28	0.67	0.32	0.65	0.45	0.31	0.81
MCD [23]	0.27	0.69	0.27	0.65	0.33	0.46	0.33	0.2	0.76
OCSVM [24]	0.26	0.67	0.23	0.61	0.28	0.48	0.41	0.3	0.8
Donut [25]	0.26	0.71	0.2	0.64	0.28	0.52	0.36	0.21	0.81
RobustPCA [26]	0.24	0.61	0.24	0.58	0.29	0.6	0.42	0.33	0.81
FITS [27]	0.21	0.66	0.15	0.58	0.22	0.72	0.32	0.16	0.81
OFA [28]	0.21	0.63	0.15	0.55	0.21	0.72	0.41	0.17	0.83
EIF [29]	0.21	0.71	0.19	0.67	0.26	0.74	0.44	0.26	0.81
COPOD [11]	0.2	0.69	0.2	0.65	0.27	0.72	0.41	0.24	0.8
IForest [30]	0.2	0.69	0.19	0.66	0.26	0.68	0.41	0.24	0.8
HBOS [31]	0.19	0.67	0.16	0.63	0.24	0.67	0.4	0.24	0.8
TimesNet [32]	0.19	0.64	0.13	0.56	0.2	0.68	0.32	0.17	0.82
KNN [33]	0.18	0.59	0.14	0.51	0.19	0.69	0.45	0.21	0.79
TranAD [4]	0.18	0.65	0.14	0.59	0.21	0.68	0.4	0.21	0.79
LOF [34]	0.14	0.6	0.1	0.53	0.15	0.57	0.32	0.14	0.76
AnomalyTransformer [5]	0.12	0.57	0.07	0.52	0.12	0.53	0.33	0.14	0.74

TABLE III

COMPARISON OF OUR PROPOSED METHOD WITH ITS CLOSER BASELINE, LSTMAD, THE BEST OTHER PERFORMING MODEL, CNN, AND A MODEL RETURNING RANDOM PREDICTIONS (RAND). WE PRESENT THE RESULTS FOR THE TWO MOST COMPREHENSIVE METRICS, VUS-PR AND VUS-AUC. OUR METHOD IS PRESENTED IN TWO VARIANTS: RECONSTRUCTION (NOTED AS **R**) AND FORECASTING (NOTED AS **F**) WITH TWO LOSSES: **MSE** AND **SOFTDTW** (NOTED AS **DTW**). THE BEST-PERFORMING METHOD FOR EACH METRIC AND DATASET IS MARKED IN BOLD.

Dataset	VUS-PR							VUS-ROC						
	R(MSE)	R(DTW)	F(MSE)	F(DTW)	LSTMAD	CNN	Rand	R(MSE)	R(DTW)	F(MSE)	F(DTW)	LSTM	CNN	Rand
CATSV2 [35]	0.10	0.10	0.04	0.04	0.04	0.08	0.03	0.61	0.61	0.46	0.46	0.43	0.64	0.53
CreditCard [36]	0.06	0.07	0.02	0.02	0.02	0.02	0.02	0.75	0.81	0.87	0.87	0.87	0.86	0.84
Daphnet [37]	0.50	0.46	0.31	0.31	0.31	0.21	0.06	0.95	0.95	0.81	0.81	0.81	0.84	0.52
Exathlon [38]	0.91	0.91	0.82	0.82	0.82	0.68	0.10	0.95	0.95	0.89	0.89	0.89	0.88	0.51
GECCO [39]	0.04	0.04	0.02	0.02	0.02	0.03	0.02	0.50	0.54	0.44	0.44	0.44	0.65	0.64
GHL [40]	0.01	0.01	0.16	0.16	0.06	0.02	0.01	0.46	0.45	0.69	0.68	0.63	0.55	0.52
Genesis [41]	0.01	0.01	0.03	0.03	0.04	0.10	0.01	0.78	0.85	0.58	0.58	0.58	0.96	0.77
LTDB [42]	0.40	0.34	0.34	0.34	0.31	0.33	0.19	0.70	0.68	0.71	0.71	0.71	0.72	0.58
MITDB [42]	0.09	0.08	0.13	0.13	0.11	0.14	0.04	0.66	0.66	0.69	0.68	0.67	0.69	0.54
MSL [43]	0.38	0.40	0.41	0.34	0.23	0.35	0.08	0.81	0.81	0.81	0.77	0.73	0.77	0.63
OPPORT. [44]	0.16	0.16	0.16	0.16	0.17	0.16	0.05	0.28	0.28	0.65	0.65	0.65	0.61	0.53
PSM [45]	0.18	0.18	0.24	0.24	0.22	0.22	0.13	0.61	0.62	0.74	0.73	0.72	0.70	0.54
SMAP [43]	0.35	0.32	0.20	0.22	0.17	0.20	0.04	0.73	0.74	0.76	0.76	0.71	0.78	0.60
SMD [13]	0.35	0.37	0.31	0.30	0.31	0.37	0.05	0.83	0.84	0.83	0.83	0.83	0.83	0.60
SVDB [46]	0.26	0.19	0.20	0.20	0.15	0.19	0.06	0.68	0.67	0.72	0.72	0.69	0.73	0.57
SWaT [47]	0.34	0.35	0.16	0.16	0.16	0.48	0.14	0.71	0.71	0.50	0.50	0.47	0.74	0.53
TAO [48]	0.80	0.82	1.00	1.00	0.99	1.00	0.77	0.88	0.91	1.00	1.00	1.00	1.00	0.94

indicating robust performance across both classical detection (AUC-PR/ROC) and other anomaly detection metrics.

Although CNN and LSTMAD are competitive in some individual metrics (e.g., CNN reaches Event-based-F1 of 0.65), they are consistently lower than xLSTMAD-F in overall anomaly structure modeling. Notably, classical methods such

as PCA, IForest, or AutoEncoder perform significantly worse across all detection metrics.

These results highlight the strength of xLSTMAD on this challenging multivariate anomaly detection benchmark (**RQ1**).

B. Fine-grained anomaly detection results

Table III shows the fine-grained results for each of the 17 datasets from the TSB-AD-M benchmark, where our proposed xLSTMAD method is compared in its four variants (xLSTMAD-R MSE, xLSTMAD-R SoftDTW, xLSTM-F MSE, xLSTMAD-F SoftDTW) against the top-performing methods in the general results across multiple datasets (LSTM, CNN). This allows us to achieve a fine-grained view of model performance on specific datasets, discarding low-performing baselines. In addition to anomaly detection baselines, we display performance obtained with the Random model (Rand) as a reference point for random performance. Its VUS-PR scores are close to zero for most datasets, with the exception of TAO.

The results show that our models consistently outperform the LSTM and CNN baselines across most data sets in both VUS-PR and VUS-ROC. Notably, xLSTMAD-R often dominates in VUS-PR, while xLSTMAD-F shines in VUS-ROC, suggesting complementary strengths between reconstruction and prediction-based detection. On *industrial datasets* such as Exathlon, SMD, and SWaT, our models achieve strong performance, with xLSTMAD-R matching or exceeding baselines for both MSE and SoftDTW loss. For Exathlon, xLSTMAD-R (SoftDTW) reaches a near-perfect VUS-PR of 0.91 and VUS-ROC of 0.95. In *physiological datasets* like Daphnet, MITDB, and LTDB, our models show notable improvements.

On Daphnet, xLSTMAD-R (MSE) achieves a VUS-PR of 0.50 compared to 0.31 for LSTM and 0.21 for CNN. On *high-noise or sparse* anomaly datasets such as CATSv2 and GECCO, the performance margins are smaller, though xLSTMAD-R (SoftDTW) still outperforms CNN and LSTM in most cases. On the other hand, all variants of xLSTMAD achieve very low VUS-PR results for the Genesis dataset. The reason behind such results may be the fact that the Genesis dataset consists of just three very short anomalies [1]. The *TAO dataset* is a notable example with perfect or near-perfect scores across all models. All four variants of our approach achieve VUS-ROC = 1.00 and two of them achieve VUS-PR = 1.00 xLSTMAD-F, indicating the ease of detecting anomalies in this scenario.

In summary, the proposed xLSTM-based methods consistently demonstrate high detection capability across various domains, delivering the best results in terms of VUS-PR in 14 of 17 datasets (RQ2).

VI. CONCLUSION

In this paper, we propose xLSTMAD, the first method that integrates a full encoder-decoder xLSTM architecture, purpose-built for multivariate time series anomaly detection. Following the two most adopted types of approach to anomaly detection, our method is designed in two variants: forecasting xLSTMAD-F and reconstruction xLSTMAD-R, which provide a high degree of flexibility to different domains. Furthermore, we investigate the performance of two loss functions: Mean Squared Error (MSE), and Soft Dynamic Time Warping (SoftDTW) to consider local reconstruction fidelity and

global sequence alignment, respectively. In our results on the comprehensive TSB-AD-M benchmark, xLSTM outperforms 23 popular anomaly detection baselines, achieving state-of-the-art performance in terms of challenging metrics such as VUS-PR and VUS-ROC.

As future work, we aim to further study xLSTM modeling capabilities in the context of anomaly detection, leading to new model architectures that are capable of providing a more balanced performance-efficiency tradeoff.

REFERENCES

- [1] Q. Liu and J. Paparrizos, "The elephant in the room: Towards a reliable time-series anomaly detection benchmark," *Advances in Neural Information Processing Systems*, vol. 37, pp. 108 231–108 261, 2024.
- [2] M. Munir, S. A. Siddiqui, A. Dengel, and S. Ahmed, "Deepant: A deep learning approach for unsupervised anomaly detection in time series," *Ieee Access*, vol. 7, pp. 1991–2005, 2018.
- [3] Z. Ji, J. Gong, and J. Feng, "A novel deep learning approach for anomaly detection of time series data," *Scientific Programming*, vol. 2021, no. 1, p. 6636270, 2021.
- [4] S. Tuli, G. Casale, and N. R. Jennings, "Tranad: deep transformer networks for anomaly detection in multivariate time series data," *Proceedings of the VLDB Endowment*, vol. 15, no. 6, pp. 1201–1214, 2022.
- [5] J. Xu, H. Wu, J. Wang, and M. Long, "Anomaly transformer: Time series anomaly detection with association discrepancy," in *International Conference on Learning Representations*.
- [6] M. Beck, K. Pöppel, M. Spanring, A. Auer, O. Prudnikova, M. Kopp, G. Klambauer, J. Brandstetter, and S. Hochreiter, "xlstm: Extended long short-term memory," *Advances in Neural Information Processing Systems*, vol. 37, pp. 107 547–107 603, 2025.
- [7] A. Auer, P. Podest, D. Klotz, S. Böck, G. Klambauer, and S. Hochreiter, "Tirex: Zero-shot forecasting across long and short horizons with enhanced in-context learning," 2025.
- [8] H. Ma, H. Sun, L. Yi, X. Liu, and G. Wang, "Multi-source data lossless compression via parallel expansion mapping and xlstm," in *ICASSP 2025-2025 IEEE International Conference on Acoustics, Speech and Signal Processing (ICASSP)*. IEEE, 2025, pp. 1–5.
- [9] M. Beck, K. Pöppel, P. Lippe, R. Kurle, P. M. Blies, G. Klambauer, S. Böck, and S. Hochreiter, "xlstm 7b: A recurrent llm for fast and efficient inference," in *ICLR 2025 Workshop on Foundation Models in the Wild*.
- [10] C. C. Aggarwal and C. C. Aggarwal, *An introduction to outlier analysis*. Springer, 2017.
- [11] Z. Li, Y. Zhao, N. Botta, C. Ionescu, and X. Hu, "Copod: copula-based outlier detection," in *2020 IEEE international conference on data mining (ICDM)*. IEEE, 2020, pp. 1118–1123.
- [12] M. Sakurada and T. Yairi, "Anomaly detection using autoencoders with nonlinear dimensionality reduction," in *Proceedings of the MLSDA 2014 2nd workshop on machine learning for sensory data analysis*, 2014, pp. 4–11.
- [13] Y. Su, Y. Zhao, C. Niu, R. Liu, W. Sun, and D. Pei, "Robust anomaly detection for multivariate time series through stochastic recurrent neural network," in *Proceedings of the 25th ACM SIGKDD international conference on knowledge discovery & data mining*, 2019, pp. 2828–2837.
- [14] X. Fan, C. Tao, and J. Zhao, "Advanced stock price prediction with xlstm-based models: Improving long-term forecasting," in *2024 11th International Conference on Soft Computing & Machine Intelligence (ISCM)*. IEEE, 2024, pp. 117–123.
- [15] B. Alkin, M. Beck, K. Pöppel, S. Hochreiter, and J. Brandstetter, "Vision-lstm: xlstm as generic vision backbone," in *First Workshop on Long-Context Foundation Models@ ICML 2024*.
- [16] M. Cuturi and M. Blondel, "Soft-dtw: A differentiable loss function for time-series," in *Proceedings of the 34th International Conference on Machine Learning*, 2017, pp. 894–903.
- [17] T. Fawcett, "An introduction to roc analysis," *Pattern recognition letters*, vol. 27, no. 8, pp. 861–874, 2006.
- [18] J. Davis and M. Goadrich, "The relationship between precision-recall and roc curves," in *Proceedings of the 23rd international conference on Machine learning*, 2006, pp. 233–240.

- [19] J. Paparrizos, P. Boniol, T. Palpanas, R. S. Tsay, A. Elmore, and M. J. Franklin, "Volume under the surface: a new accuracy evaluation measure for time-series anomaly detection," *Proceedings of the VLDB Endowment*, vol. 15, no. 11, pp. 2774–2787, 2022.
- [20] J. Audibert, P. Michiardi, F. Guyard, S. Marti, and M. A. Zuluaga, "Usad: Unsupervised anomaly detection on multivariate time series," in *Proceedings of the 26th ACM SIGKDD international conference on knowledge discovery & data mining*, 2020, pp. 3395–3404.
- [21] T. Yairi, Y. Kato, and K. Hori, "Fault detection by mining association rules from house-keeping data," in *proceedings of the 6th International Symposium on Artificial Intelligence, Robotics and Automation in Space*, vol. 18. Citeseer, 2001, p. 21.
- [22] Z. He, X. Xu, and S. Deng, "Discovering cluster-based local outliers," *Pattern recognition letters*, vol. 24, no. 9-10, pp. 1641–1650, 2003.
- [23] D. EStimator, "A fast algorithm for the minimum covariance," *Technometrics*, vol. 41, no. 3, p. 212, 1999.
- [24] M. Hejazi and Y. P. Singh, "One-class support vector machines approach to anomaly detection," *Applied Artificial Intelligence*, vol. 27, no. 5, pp. 351–366, 2013.
- [25] H. Xu, W. Chen, N. Zhao, Z. Li, J. Bu, Z. Li, Y. Liu, Y. Zhao, D. Pei, Y. Feng *et al.*, "Unsupervised anomaly detection via variational auto-encoder for seasonal kpis in web applications," in *Proceedings of the 2018 world wide web conference*, 2018, pp. 187–196.
- [26] R. Paffenroth, K. Kay, and L. Servi, "Robust pca for anomaly detection in cyber networks," *arXiv preprint arXiv:1801.01571*, 2018.
- [27] Z. Xu, A. Zeng, and Q. Xu, "Fits: Modeling time series with 10k parameters," in *The Twelfth International Conference on Learning Representations*.
- [28] T. Zhou, P. Niu, L. Sun, R. Jin *et al.*, "One fits all: Power general time series analysis by pretrained lm," *Advances in neural information processing systems*, vol. 36, pp. 43 322–43 355, 2023.
- [29] S. Hariri, M. C. Kind, and R. J. Brunner, "Extended isolation forest," *IEEE transactions on knowledge and data engineering*, vol. 33, no. 4, pp. 1479–1489, 2019.
- [30] F. T. Liu, K. M. Ting, and Z.-H. Zhou, "Isolation forest," in *2008 eighth ieee international conference on data mining*. IEEE, 2008, pp. 413–422.
- [31] M. Goldstein and A. Dengel, "Histogram-based outlier score (hbos): A fast unsupervised anomaly detection algorithm," *KI-2012: poster and demo track*, vol. 1, pp. 59–63, 2012.
- [32] H. Wu, T. Hu, Y. Liu, H. Zhou, J. Wang, and M. Long, "Timesnet: Temporal 2d-variation modeling for general time series analysis," in *The Eleventh International Conference on Learning Representations*.
- [33] S. Ramaswamy, R. Rastogi, and K. Shim, "Efficient algorithms for mining outliers from large data sets," in *Proceedings of the 2000 ACM SIGMOD international conference on Management of data*, 2000, pp. 427–438.
- [34] M. M. Breunig, H.-P. Kriegel, R. T. Ng, and J. Sander, "Lof: identifying density-based local outliers," in *Proceedings of the 2000 ACM SIGMOD international conference on Management of data*, 2000, pp. 93–104.
- [35] P. Fleith, "Controlled anomalies time series (cats) dataset."
- [36] I. Sharafaldin, A. H. Lashkari, A. A. Ghorbani *et al.*, "Toward generating a new intrusion detection dataset and intrusion traffic characterization," *ICISSp*, vol. 1, no. 2018, pp. 108–116, 2018.
- [37] M. Bachlin, M. Plotnik, D. Roggen, I. Maidan, J. M. Hausdorff, N. Giladi, and G. Troster, "Wearable assistant for parkinson's disease patients with the freezing of gait symptom," *IEEE Transactions on Information Technology in Biomedicine*, vol. 14, no. 2, pp. 436–446, 2009.
- [38] V. Jacob, F. Song, A. Stiegler, B. Rad, Y. Diao, and N. Tatbul, "Exathlon: A benchmark for explainable anomaly detection over time series," *arXiv preprint arXiv:2010.05073*, 2020.
- [39] S. Moritz, F. Rehbach, S. Chandrasekaran, M. Rebolledo, and T. Bartz-Beielstein, "Gecco industrial challenge 2018 dataset: A water quality dataset for the 'internet of things: Online anomaly detection for drinking water quality' competition at the genetic and evolutionary computation conference 2018, kyoto, japan," *Kyoto, Japan*, 2018.
- [40] P. Filonov, A. Lavrentyev, and A. Vorontsov, "Multivariate industrial time series with cyber-attack simulation: Fault detection using an lstm-based predictive data model," *arXiv preprint arXiv:1612.06676*, 2016.
- [41] A. von Birgelen and O. Niggemann, "Anomaly detection and localization for cyber-physical production systems with self-organizing maps," in *IMPROVE-Innovative Modelling Approaches for Production Systems to Raise Validatable Efficiency: Intelligent Methods for the Factory of the Future*. Springer Berlin Heidelberg Berlin, Heidelberg, 2018, pp. 55–71.
- [42] A. L. Goldberger, L. A. Amaral, L. Glass, J. M. Hausdorff, P. C. Ivanov, R. G. Mark, J. E. Mietus, G. B. Moody, C.-K. Peng, and H. E. Stanley, "Physiobank, physiotookit, and physionet: components of a new research resource for complex physiologic signals," *circulation*, vol. 101, no. 23, pp. e215–e220, 2000.
- [43] K. Hundman, V. Constantinou, C. Laporte, I. Colwell, and T. Soderstrom, "Detecting spacecraft anomalies using lstms and nonparametric dynamic thresholding," in *Proceedings of the 24th ACM SIGKDD international conference on knowledge discovery & data mining*, 2018, pp. 387–395.
- [44] D. Roggen, A. Calatroni, M. Rossi, T. Holleczeck, K. Förster, G. Tröster, P. Lukowicz, D. Bannach, G. Pirkel, A. Ferscha *et al.*, "Collecting complex activity datasets in highly rich networked sensor environments," in *2010 Seventh international conference on networked sensing systems (INSS)*. IEEE, 2010, pp. 233–240.
- [45] A. Abdulaal, Z. Liu, and T. Lancewicki, "Practical approach to asynchronous multivariate time series anomaly detection and localization," in *Proceedings of the 27th ACM SIGKDD conference on knowledge discovery & data mining*, 2021, pp. 2485–2494.
- [46] S. D. Greenwald, R. S. Patil, and R. G. Mark, *Improved detection and classification of arrhythmias in noise-corrupted electrocardiograms using contextual information*. IEEE, 1990.
- [47] A. P. Mathur and N. O. Tippenhauer, "Swat: A water treatment testbed for research and training on ics security," in *2016 international workshop on cyber-physical systems for smart water networks (CySWater)*. IEEE, 2016, pp. 31–36.
- [48] TAO. [Online]. Available: <https://www.pmel.noaa.gov/>